Journal of Biological Physics (2021) 47:79–93
https://doi.org/10.1007/s10867-021-09566-9

ORIGINAL PAPER

Orientational dynamics of magnetotactic bacteria in Earth's magnetic field—a simulation study

Savitha Satyanarayana, et al. *[full author details at the end of the article]*

Received: 3 January 2020 / Accepted: 4 February 2021 / Published online: 9 March 2021

Abstract
We investigate through simulations the phenomena of magnetoreception to enable an understanding of the minimum requirements of a fail-safe mechanism, operational at the cellular level, to sense a weak magnetic field at ambient temperature in a biologically active environment. To do this, we use magnetotactic bacteria (MTB) as our model system. The magnetic field sensing ability of these bacteria is due to the presence of magnetosomes, which are internal membrane-bound organelles that contain an iron-based magnetic mineral crystal. These magnetosomes are usually found arranged in a chain aligned with the long axis of the bacterial body. This arrangement yields an overall magnetic dipole moment to the bacterial cell. To simulate this orientation process, we set up a rotational Langevin stochastic differential equation and solve it repeatedly over appropriate time steps for isolated spherical shaped MTB as well as for a more realistic model of spheroidal MTB with flagella. The orientation process appears to depend on shape parameters with spheroidal MTB showing a slower response time compared to spherical MTB. Further, our simulation also reveals that the alignment to the external magnetic field is more robust for an MTB when compared to single magnetosome. For the simulation involving magnetosomes, we include an extra torque that arises from the twisting of an attachment tether and enhance the viscosity of the surrounding medium to mimic intracellular conditions in the governing Langevin equation. The response time of alignment is found to be substantially reduced when one includes a dipole interaction term with a neighboring magnetosome and the alignment becomes less robust with increase in inter dipole distance. The alignment process can thereby be said to be very sensitively dependent on the distance between magnetosomes. Simulating the process of alignment between two neighboring magnetosomes, both in the absence and presence of an ambient magnetic field, we conclude that alignment between these dipoles at the distances typical in an MTB is highly probable and it would be the locked unit that responds to changes in the external magnetic field.

Keywords Navigation · Magnetoreception · Stochastic equation · Orientation process · Dipole interaction · Relaxation time

1 Introduction

Many organisms have the capability of sensing Earth's magnetic field. Magnetotactic bacteria (MTB), discovered by Richard P. Blakemore in 1970 [1], are some of the simplest life forms that demonstrate this capacity of magnetic field sensing. These bacteria use this capacity to navigate along geomagnetic field lines. The ability to sense a magnetic field is due to the presence of magnetosomes, which are membrane-bound organelles containing an iron-based magnetic material. The magnetosomes are also responsible for the biomineralization of this material. MTB are, in general, found to contain 10–20 cuboidal or octahedral magnetosomes, each of which consists of a magnetic nanoparticle, either magnetite (Fe_3O_4) or greigite (Fe_3S_4) which is enveloped by a lipid bilayer membrane [2, 3]. The magnetosome membrane contains a number of proteins like Mam A, Mam B, Mam J, and Mam K which are unique to MTB [4]. The magnetic nanoparticle sizes are usually within the single magnetic domain size limit having lengths in the range 35–120 nm [5]. The magnetosomes are aligned in a chain-like fashion along the long axis of the bacterial body attached to the magnetosome filament via the magnetosome connector Mam J. Andre Kornig et al. [6] report on the mechanical properties of the magnetosomes attached to the cytoskeletal filament via the magnetosome connector. They report that magnetosome chains are extremely stable up to a field strength of 30 mT which is about 500 times the strength of the geomagnetic field. Kiani et al. [7] conclude that the presence of a filament is vital for the formation of the linear magnetosome chain observed in MTB. Further, in the case of weaker external fields like the Earth's magnetic field, they report that nearest neighbor interactions dominate, favoring the formation of a single chain rather than multiple short chains. This arrangement of chain formation imparts a magnetic dipole moment to the bacterial cell as a whole. This dipole moment interacts with the external magnetic field (Earth's field or any other applied field) producing a torque which aligns the cell along the field lines. This phenomenon is called magnetotaxis and led Blakemore to name the bacteria displaying this ability as magnetotactic bacteria. Magnetotaxis only implies that the magnetic field influences the swimming direction but not the absolute velocity of the cells [1]. For movement, MTB have a flagellum, which is used for self-propulsion [1]. The magnetosomes are essentially fixed in both position and orientation within the whole cell after an alignment with the Earth's magnetic field due to the high effective viscosity of the cytoplasm as reported by S. Ofer et al. [8]. Various morphologies of MTB, such as rods, vibrio, spiral, cocci, and multicellular bacteria, have been found.

The fact that many higher creatures (insects, mollusks, fish, amphibians, reptiles, birds, and mammals) are able to navigate by sensing Earth's magnetic field has been well documented [9]. However the sensor and sensory mechanism are still elusive to the scientific community and therefore are of great research interest. The magnetic sensing capabilities in higher creatures suggests that they biomineralize single magnetic domain Fe_3O_4 crystals of morphologies that are similar to that found in MTB [10]. Models for magnetic particle-based magnetoreception (MPM) in higher animals have been described in [11]. The mechanism hypothesized involves the presence of magnetic nanoparticles in certain sensor cells either as superparamagnetic clusters or linear chains attached with cytoskeletal filaments to either mechanosensitive ion channels or force-gated ion channels on the cell membrane. A torque generated by the reorientation of these magnetic entities to an ambient magnetic field would cause ion channel activation either directly or through a secondary messenger. This would lead to cell depolarization developing an action potential which traveling via the nervous system would finally trigger a neuronal response in the brain. Understanding the underlying principles

in magnetic sensing mechanism and factors affecting the process of alignment with the magnetic field in MTB could help us in comprehending the basis for magnetoreception in higher organisms.

Using MTB as a model system, we investigate through simulations the phenomena of magnetoreception seen at the cellular level in living organisms. It is obvious that MTB have a fail-safe mechanism of sensing a weak magnetic field at ambient temperature in a biologically active and thereby extremely noisy environment. We wish to arrive at an understanding of the basic requirements for a robust magneto-sensing capacity under such conditions. The ultimate aim would be an ability to predict via simulation studies the minimum number of magnetosomes that would be required for this as a function of the magnetic moment of each magnetosome, local magnetic field strength, ambient temperature, viscosity of the surrounding medium, and the rigidity modulus of the tether that fixes the spatial position of the magnetosome within the cell.

Note that MTB by themselves have several interesting applications in the field of geology, medicine, astrobiology, and paleontology. MTB are useful in biogeochemical cycling of iron and sulfur. In medicine, they find potential applications in drug delivery, hyperthermia, and also as contrast agents [12]. Being biocompatible in addition to possessing magnetic sensing capabilities, they can be guided using an external magnetic field to the area of a tumor to deliver drugs to the specific point in the organ, avoiding potential hazards to the other organs of the body. However, these applications have not yet been developed commercially, mainly because MTB are difficult to cultivate in large numbers due to their fastidious nature [13]. Simulation studies could help us arrive at synthetic alternative mechanisms that are capable of performing equivalently for such applications but are easier to fabricate and more commercially viable.

2 Modeling details

2.1 Alignment of an isolated magnetotactic bacterium to Earth's magnetic field

The average orientation of a cell with respect to the direction of the local magnetic field is determined by the ratio of the energy lowered when there is complete alignment of the magnetic moment of the bacterium with the magnetic field to the thermal energy, $\frac{MB}{k_BT}$.Here M is the magnitude of the magnetic moment on the cell; B, the strength of the Earth's magnetic field while the factor k_BT is linked to the random forces associated with Brownian motion that tend to randomize the cell orientation, k_B being the Boltzmann constant and T the ambient temperature. The mean alignment of swimming MTB in water is given by the Langevin function for classical paramagnetism,

$$\langle cos\theta \rangle = L\left(\frac{MB}{k_BT}\right) \tag{1}$$

where θ is the angle between the directions of cell magnetic moment ($\overrightarrow{\boldsymbol{M}}$) and the magnetic field ($\overrightarrow{\boldsymbol{B}}$) [1] while $L(x) = coth(x) - \frac{1}{x}$ is the Langevin function.

To set up a Langevin stochastic differential equation for the process of alignment of $\overrightarrow{M}$ with $\overrightarrow{B}$, a single bacterium of magnetic moment $\overrightarrow{M}$, which is assumed to be spherical in shape with a radius of R, is considered. In addition to the magnetic alignment torque arising from the interaction of $\overrightarrow{M}$ with $\overrightarrow{B}$, the MTB is affected by a drag torque $\gamma\dot{\theta}$, where $\gamma = 8\pi\eta R^3$ is the rotational frictional drag coefficient with η being the viscosity of the surrounding medium (water), as well as a Brownian motion induced torque $\tau(t)$ arising from collisions with the surrounding water molecules. Neglecting the inertial term here as this is in a low Reynolds number regime [14], the rotational equation of motion can be written as

$$MBsin\theta + 8\pi\eta R^3 \frac{d\theta}{dt} + \tau(t) = 0. \tag{2}$$

The Brownian motion induced torque due to thermal effects is denoted by $\tau(t)$ and can be written as $\sqrt{2k_BT\gamma}\frac{w_i}{\sqrt{dt}}$, where w_i are uncorrelated random numbers with a mean of zero, unit variance, and Gaussian probability distribution [15], while dt is a small time interval step that is taken to be one thousandth of the characteristic Brownian relaxation time of the cell. The Brownian relaxation time is given by $t_B = \frac{3\eta V}{k_BT}$, where V is the volume of the particle [16]. Note that the alignment process is assumed to take place in the plane containing $\overrightarrow{M}$ and $\overrightarrow{B}$ and the effect of the random Brownian generated torque is only considered in the plane in which the alignment takes place.

To simulate a situation closer to that in real life, the Langevin stochastic differential equation is modified to account for a spheroidal body shape for the MTB as well as the effect of motion of a single flagellum. Here too, the effect of the flagellar motion is considered only in the plane in which the alignment takes place and can be thus reduced to a sinusoidally varying term. The equation can be thus written as

$$MB\sin\theta + \gamma\frac{d\theta}{dt} + aF\sin\omega t + \tau(t) = 0 \tag{3}$$

where $\gamma = 8\pi\eta ab^2\gamma_p$, $\gamma_p = \frac{4}{3}\left\{\frac{\left(\frac{b^2}{a^2}-\frac{a^2}{b^2}\right)}{\left[2-\beta\left(2-\frac{b^2}{a^2}\right)\right]}\right\}$, $\beta = \frac{2tanh^{-1}e}{e}$ and $e = \frac{\sqrt{\frac{a^2}{b^2}-1}}{\frac{a}{b}}$ is the eccentricity of the spheroid, a and b being the major and minor axis of the spheroid respectively, F the magnitude of the flagellar driving force, and ω, the angular frequency of rotation of the flagella attached to the bacteria [17].

2.2 Alignment of an isolated spherical magnetosome in Earth's magnetic field

A single spherical magnetosome in addition to the magnetic alignment torque experiences a viscous drag torque due to viscosity of the cytoplasm and a restoring couple exerted by the attachment tether filament. The rotational equation of motion can be written as

$$MBsin\theta + \gamma\frac{d\theta}{dt} + c\theta + \tau(t) = 0. \tag{4}$$

Here M stands for the magnetic moment of magnetosome; $\gamma = 8\pi\eta R^3$ where η is now the effective viscosity of the cytoplasm of the MTB; R, the radius of the magnetosome; c, the restoring couple per unit twist of the attachment tether; and $\tau(t)$, the Brownian motion induced torque experienced by the magnetosome within the cell volume.

2.3 Effect of dipole interaction with a neighboring magnetosome on the alignment process

Two neighboring magnetosomes are treated as two interacting dipoles separated by a distance, s. The magetosomes are treated as point dipoles and the distance between the centers of the two dipoles is taken to be 50 nm as reported by Bahareh Kiani et al. [7]. The alignment torque between the two magnetic dipoles is given by the following expression [4]:

$$\overrightarrow{T}_{ab} = \frac{\mu_0 m_a m_b}{4\pi s^3}\left[3\left(\widehat{m}_a.\widehat{s}\right)\left(\widehat{m}_b \times \widehat{s}\right) + \left(\widehat{m}_a \times \widehat{m}_b\right)\right] \tag{5}$$

where $\overrightarrow{m}_a = m_a\ \widehat{m}_a$ and $\overrightarrow{m}_b = m_b\ \widehat{m}_b$ are two point-like neighboring magnetic dipoles separated by a distance s. If the two magnetic moments are of the same magnitude, then m_a and m_b are replaced by $|M|$. Equation (5) can be written in terms of the angles, θ and θ_1, the two neighboring dipoles make with the Earth's magnetic field, assuming that all three of them are contained in a plane, as

$$T = \frac{\mu_0 |M|^2}{4\pi s^3}[3sin\theta cos\theta_1 + \sin(\theta_1 - \theta)] \tag{6}$$

The dipole interaction torque (6) is included in the Langevin stochastic differential equation as shown below:

$$MBsin\theta + \gamma\frac{d\theta}{dt} + c\theta + \tau(t) + \frac{\mu_0 |M|^2}{4\pi s^3}[3sin\theta cos\theta_1 + \sin(\theta_1 - \theta)] = 0 \tag{7}$$

A similar equation is written for θ_1 as shown below:

$$MBsin\theta_1 + \gamma\frac{d\theta_1}{dt} + c\theta_1 + \tau(t) + \frac{\mu_0 |M|^2}{4\pi s^3}[3sin\theta_1 cos\theta + \sin(\theta - \theta_1)] = 0 \tag{8}$$

Equations (7) and (8) are solved together to find the variation of θ and θ_1 with time.

Three different cases are considered:

1. The dipoles are always parallel to each other. That is, $\theta = \theta_1$. Here individual alignment response to the external field is eliminated.
2. The angular position of one dipole is fixed thus allowing no response to any torques while the angular position of the other dipole is influenced by the magnetic moment due to the fixed dipole, the external magnetic field, as well as the random torques generated due to Brownian motion in the surroundings.
3. The most general case where both dipoles try to align with the external field simultaneously and both the angles θ and θ_1 change continuously. This is handled by allowing evolution of θ for a small time step dt keeping θ_1 constant. The value of θ at the end of dt is then incorporated into the governing differential equation for θ_1. This is then held constant while θ_1 is evolved for a time dt. The process is then repeated, allowing for a "pseudo" simultaneous evolution of both θ and θ_1. Here each dipole is influenced by the magnetic moment of the other dipole, the external ambient magnetic field, as well as the Brownian motion generated torque on each dipole.

3 Results and discussion

3.1 Alignment of isolated spherical MTB with the Earth's magnetic field

Taking $M = 2.2 \times 10^{-15} Am^2$, $B = 50 \times 10^{-6}\ T$, $\eta = 0.89 \times 10^{-3}\ Pa.s$, $T = 300K$ and $R = 1.2 \times 10^{-6} m$, [14], Eq. (2) is used to generate the variation of θ with time and is shown in Fig. 1 in red. The analytical solution of Eq. (2) has the form

$$\theta(t) = 2tan^{-1}\left\{ tan\frac{\theta_0}{2}\, e^{-t/t_{ch}} \right\} \tag{9}$$

where θ_0 is the initial angle at time $t = 0$ while $t_{ch} = \frac{\gamma}{MB}$ can be called the characteristic time. At the low angle range, using small angle approximation, $sin\theta \sim \theta$, the analytical solution to Eq. (2), ignoring the thermally generated noise, takes on the form

$$\theta(t) = \theta_0\, e^{-t/t_r} \tag{10}$$

where t_r is the relaxation time. Further, it can be seen that analytically $t_{ch} = t_r$. The variation in $\theta(t)$ is fitted to the form given in Eq. (9) for various initial angles θ_0 and t_{ch} is extracted. For the small angle range $\left(\theta < {}^{\pi}/_{6}\right)$ where the thermal term dominates, the average of twenty simulated reorientation processes at each initial angle is fitted to the form given in Eq. (10) and t_r is extracted. The values of t_{ch} and t_r for different initial angles are shown in Table 1. It can be seen that the values of t_{ch} and t_r match each other and are independent of the initial angle θ_0.

The relaxation time, t_r (or t_{ch}), is taken to be a gauge of the alignment response of the system, a small t_r representing a fast response while a large one represents a sluggish one. Further, the variance (the average of the squared deviations from the mean) in angle of orientation $\theta(t)$ for times greater than $t \sim 4t_r$, $\left(\sigma_a^2\right)$, is taken to be a measure of the robustness of alignment of the MTB under ambient conditions with evolution of time.

3.2 Effect of variation of external magnetic field on the alignment of MTB with field direction

The alignment process is now simulated using Eq. (2) for different values of B for a fixed initial angle $\theta_0 = {}^{\pi}/_{2}$. The variation in relaxation time (t_r) and variance in $\theta(t)$ for times greater

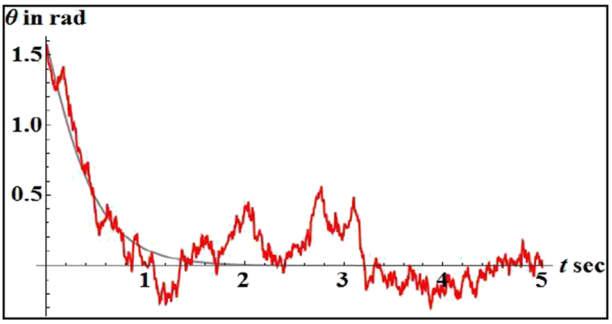

Fig. 1 Variation of angle of orientation of spherical MTB w.r.t the Earth's magnetic field direction as a function of time. Initial angle is taken as $\frac{\pi}{2}$ radians. Red line indicates variation with inclusion of thermal noise due to the surrounding system while gray is in the absence of any such noise. Relaxation time for the curve with thermal noise is 0.34 s

Table 1 Values of characteristic time t_{ch} and relaxation time t_r for various initial angles θ_0 for the alignment process of an isolated spherical MTB with the Earth's magnetic field of 50 μT. The values of t_{ch} and t_r coincide and are independent of θ_0

θ_0 (rad)	t_{ch} (s)	t_r (s)
$\pi/3$	0.36	0.35
$\pi/2$	0.34	0.34
$5\pi/2$	0.35	0.38

than $t \sim 4t_r$, (σ_a^2), with B, are shown in Fig. 2. It is clear from Fig. 2 that as the external field is increased, the increase in strength of the aligning magnetic torque decreases t_r making the alignment process a faster one while the decrease in σ_a^2 points to stronger and more robust alignment with the magnetic field direction. This is as expected. This set of simulations thus validates the use of t_r and σ_a^2 as figures of merit for the alignment process.

3.3 Alignment of an isolated spheroid-shaped flagellated MTB with the Earth's magnetic field

The simulation was repeated with a more realistic spheroidal shape for the bacterium further incorporating disturbance from the flagellar motion. Taking $a = 2.5 \times 10^{-6}$ m and $b = 0.7 \times 10^{-6}$ m as the major and minor axes, respectively, of the spheroid representing the bacterium shape, $F = 1.24 \times 10^{-13}$ N as the amplitude of the flagellar force and $\omega = 94.24$ rad s^{-1} as the angular frequency of flagellar motion [17], Eq. (3) is used to generate the variation of θ with time and this is shown in Fig. 3.

The relaxation time for spheroidal bacteria is found to be higher than that for the spherical shaped bacteria and this is as expected as the drag torque experienced by the bacterium during the alignment process is increased as a consequence of its shape. Relaxation time t_r and variance σ_a^2 for spheroidal shaped bacteria in the presence of flagellar motion are found to be

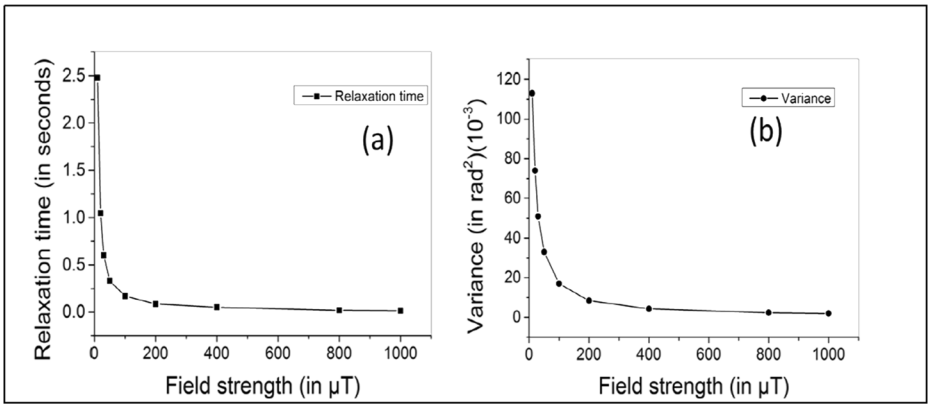

Fig. 2 Variation of (a) relaxation time t_r and (b) variance σ_a^2 in the alignment process of MTB for various strengths of external magnetic field. All simulations were carried out for the MTB making an initial angle of $\pi/2$ with the magnetic field direction

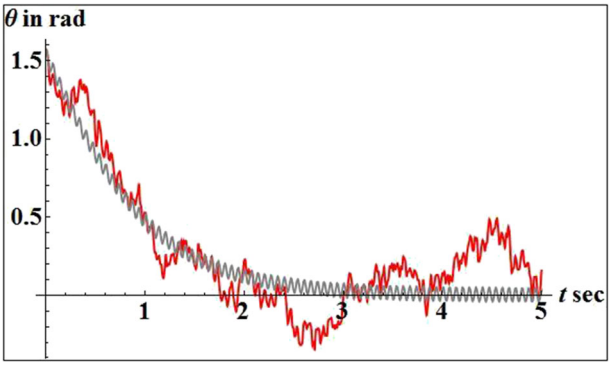

Fig. 3 Variation of angle of orientation of spheroidal shaped MTB with a single flagellum with respect to the Earth's magnetic field direction as a function of time. Initial angle is taken as $\frac{\pi}{2}$. The red line indicates variation in $\theta(t)$ with inclusion of thermal noise while the gray line is in the absence of any such noise. Relaxation time estimated for the variation with the thermally generated noise is 0.70 s

0.7 s and 0.037 rad^2, respectively. The values change to 0.72 s and 0.032 rad^2, respectively, in the absence of this additional term.

3.4 Alignment of a single magnetosome in Earth's magnetic field

Taking the values of $M = 1.6 \times 10^{-17}$Am^2 , $B = 50 \times 10^{-6}$ T , $T = 300$ K, $R = 20 \times 10^{-9}$ m, and the restoring couple of linker filament, $c = 10.6 \times 10^{-23}$N m rad^{-1} [7], Eq. (4) is used to simulate the alignment of an isolated magnetosome to the Earth's magnetic field in an intracellular environment. Note that the effective viscosity of the cytoplasm is nearly 15 times that of water [18] and the time step dt here is chosen as one hundredth of the characteristic Brownian relaxation time of the magnetosome. The resulting variation of $\theta(t)$ is shown in Fig. 4(a) and (b). The initial orientation of the magnetosome moment was taken to be $\frac{\pi}{2}$ with respect to the magnetic field. From Fig. 4(a) and (b), it is clear that a magnetosome is able to align with the field much faster than an MTB despite there being an additional tether torque that opposes the motion in case of the magnetosome.

The presence of the tether torque term in Eq. (4) also precludes any simple general analytical solution even in the absence of the thermally generated noise. Analytical solutions do exist for cases when $\frac{MB}{\gamma} \ll \frac{c}{\gamma}$ or when $\frac{MB}{\gamma} \gg \frac{c}{\gamma}$. Here, however, using appropriate values of M,

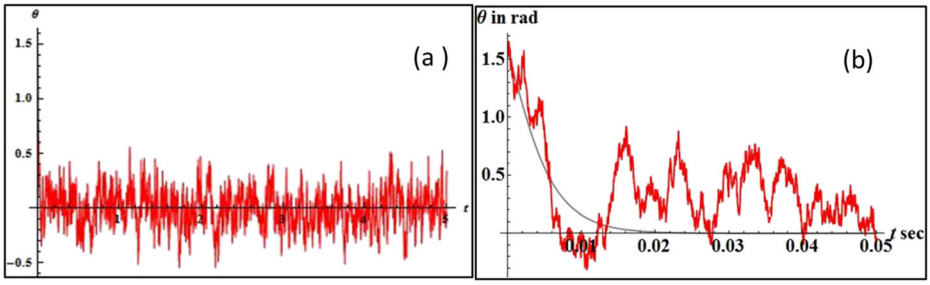

Fig. 4 Variation of angle of orientation of (a) isolated magnetosome w.r.t the Earth's magnetic field direction as a function of time (b) expanded version of graph (a) for initial times. Initial angle is taken as $\frac{\pi}{2}$ radians. Red line indicates variation with inclusion of thermal noise due to the surrounding system while gray is in the absence of any such noise. Relaxation time for the curve with thermal noise is 0.0037 s

B, R and c, one finds $\frac{MB}{\gamma} \sim 7.55 \frac{c}{\gamma}$. which fits into neither. The analytical solution for Eq. (4) with small angle approximation, however, still has the form given in Eq. (10). Thereby, as described in Section 3.1, the simulation process with initial orientation angle of $\frac{\pi}{2}$ is repeated twenty times and an average is taken for the range $\theta < {}^{\pi}/_{6}$ which is then fitted to the form given in Eq. (10) to extract t_r.

The relaxation time for a single isolated magnetosome in the presence of thermally generated noise is found to be 0.0037 s in comparison to that of 0.34 s estimated for spherical MTB. This smaller t_r can be attributed primarily to the smaller rotational drag torque in the case of the magnetosome. However, it can be seen that the orientation process is more robust for the MTB in comparison to that for a single magnetosome as σ_a^2 for spherical shaped MTB is 0.033 rad^2 while it is 0.070 rad^2 for an isolated magnetosome at a magnetic field of 50 μT.

The time of relaxation also depends on the viscosity of the cytoplasm (η) and the restoring couple per unit twist of the linker filament (c). These parameters (η and c) are varied in regular steps and the variation in the relaxation time is shown in Table 2 and Table 3. It is clear from Table 2 that as the viscosity of the cytoplasm of the cell increases, the time of relaxation t_r also increases indicating a more sluggish alignment process. The increase in the strength of the tether torque too increases t_r, as it tries to restore the magnetosome to its initial equilibrium position opposing the process of alignment with $\vec{B}$ as shown in Table 3. Note that within the reasonable range in which c is varied, from one-fourth of the experimentally estimated value to double that, σ_a^2 is not strongly affected in contrast to the case where viscosity is changed, from one-fourth of the reported value to twice that.

3.5 Effect of dipole interaction with a neighboring magnetosome on the alignment process

In cases 1 and 3, as described in Section 2.3, the dipoles simultaneously align with the field as shown in Figs. 5, 6, and 7, respectively. In case 3, the variances, σ_a^2, of the alignment process are found to be fairly insensitive to the initial relative angular positions of the two dipoles. For case 2, one finds that the free dipole tries to align with the fixed dipole rather than the ambient magnetic field direction as shown in Fig. 8**.**

From the above, we conclude that while both dipoles are influenced by the external magnetic field, they are at the same time very strongly influenced by the interaction with the other dipole and this plays a dominant role in the alignment process and thereby perhaps also in the alignment process of MTB along Earth's magnetic field direction. The variance for interacting dipoles is found to be much less than that for a single magnetosome. The value of σ_a^2 for interacting dipoles (Case 3) is 0.0003 rad^2 as compared to 0.07 rad^2 for an isolated magnetosome.

Table 2 Variation of relaxation time and variance in the alignment of a single magnetosome with the Earth's magnetic field direction for various values of cytoplasmic viscosity η keeping the couple per unit twist of the linker filament $c = 10.6 \times 10^{-23}$N m rad^{-1} and the Earth's magnetic field of 50 μT as constant parameters

η	η / c ($\times 10^{20}$) (sm^{-3}rad)	$\mathbf{t_r}$ (ms)	$\boldsymbol{\sigma_a^2}$ (in rad^2)
0.25η	0.31	0.99	0.094
0.5 η	0.63	1.87	0.076
η	1.26	3.66	0.070
1.5 η	1.89	6.43	0.057
2 η	2.52	7.62	0.043

Table 3 Variation of relaxation time t_r and variance σ_a^2 in the alignment of a single magnetosome with the Earth's magnetic field direction for various values of the couple per unit twist of the linker filament c keeping the cytoplasmic viscosity $\eta = 13.3 \times 10^{-3}$Pa.s and the Earth's magnetic field of 50 μT as constant parameters

c	η / c ($\times 10^{20}$) ($sm^{-3}rad$)	t_r (ms)	σ_a^2 (rad^2)
0.25 c	5.02	3.32	0.060
0.5c	2.51	3.42	0.062
1.0c	1.25	3.66	0.070
1.5c	0.84	4.34	0.071
2c	0.63	4.89	0.077

3.6 Effect of variation of inter-magnetic dipolar distance on the alignment of a magnetosome with the Earth's magnetic field

To investigate the importance of the distance between the two magnetosomes, the value of s, the inter-magnetic dipolar distance is varied and its effect on the robustness of alignment is measured in terms of σ_a^2. This is done by using Eq. (7) for different values of s and the results are tabulated in Table 4.

From the tabulated values, it is clear that when the inter-magnetic dipole distance is small, the variance in the angle of alignment, σ_a^2, is small but as the distance increases the variance increases implying large fluctuations from the mean alignment position. Large inter dipolar distances are not conducive to robust alignment.

3.7 Response time in (1) an alignment process of two magnetic dipoles linked with neighboring magnetosomes and (2) orientation process of a locked system of aligned magnetosomes

Since we find that a free dipole will align with a neighboring dipole that has a fixed orientation, preferentially over the ambient magnetic field, we carry out further simulations for the alignment process between two neighboring dipoles in the absence of an external magnetic field to assess the time scale of such a process. We consider two cases here: (a) when only one of the dipoles can change its orientation as a function of time and (b) when both dipoles are free. Assuming that the variation of the angle of rotation with time for a reorienting dipole can still be described by Eq. (10)

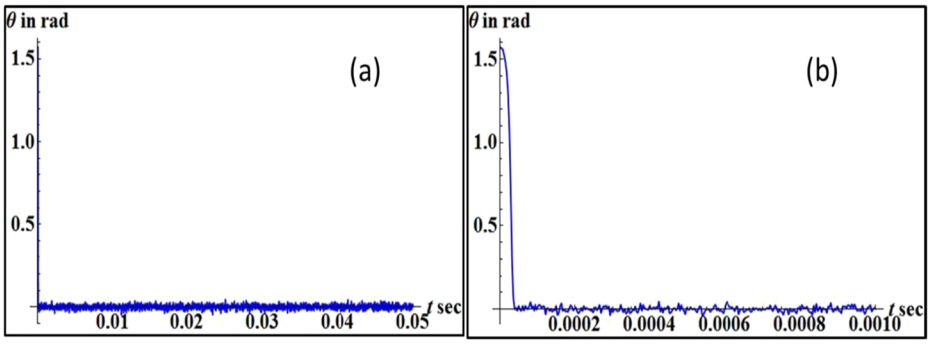

Fig. 5 (a) Variation of angle of alignment of one among a locked pair of magnetosomes (the dipoles of the two neighboring magnetosomes are assumed to be always parallel to each other due to the magnetic interaction between them) as a function of time. The initial angle is taken to be $\frac{\pi}{2}$ radians. (b) Expanded version of graph (a) for initial times (case 1)

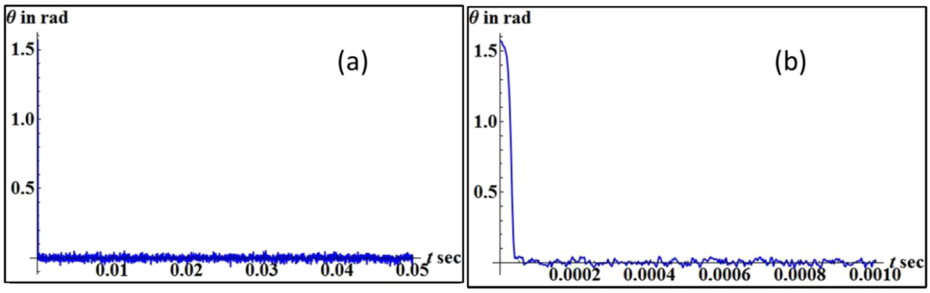

Fig. 6 (a) Variation of angle of alignment $\theta(t)$ of one magnetosome with time considering magnetic interaction with a single neighboring dipole with $\theta(0) = \frac{\pi}{2}$ radians. Each dipole is influenced by magnetic interaction with the other dipole, the external magnetic field, as well as disruption in alignment due to thermal noise. They undergo the overall alignment process simultaneously. (b) Expanded version of graph (a) for initial times. The initial angle between the two dipoles is taken to be $\frac{\pi}{6}$ radians (case 3)

in the small angle approximation, we extract values of relaxation time and variance and compare these with the values of the same when an ambient magnetic field is present. We find that while initial conditions do have an effect on the exact value of the relaxation times for both cases (a) and (b), these times are all in the order of a few microseconds whether in the absence or presence of an ambient magnetic field and the variance values are comparable. For instance, the relaxation time for case (a) when the initial angle between the two dipoles is $^{\pi}/_{3}$ is (4.29 ± 0.37) μs, in the absence of an external field (with a variance of 0.00022 rad^2) and (1.53 ± 0.13) μs with a variance of 0.00045 rad^2 in an external magnetic field. Similarly, for case (b), the relaxation time without an external magnetic field is (3.78 ± 0.25) μs with a variance of 0.00018 rad^2 and (6.21 ± 0.42) μs with a variance of 0.0003 rad^2 when the field is present. As the response time for the orientation process of a dipole, be it an alignment with a neighboring dipole (fixed or free) or to an external field, is approximately the same, we conclude that alignment between neighboring dipoles is inevitable and one can expect that it will be the locked system of the two dipoles that respond as a whole to an ambient magnetic field.

Given this, we have extended our simulations further to study the response of a locked system of magnetic dipoles (multiple magnetosomes in the case of the model system being considered here) to the Earth's magnetic field. We assume that the magnetosomes arrange themselves in a rigid linear chain, the dipoles aligning along the axis of this chain [3], which then reorients to align with the ambient field direction. Taking the length of this rigid chain to be multiples of the inter magnetosome distance d, as reported in [7], we attribute to it a rotational drag of a cylinder with length $l = (n-1) \times d + 2R$ and diameter $2R$, where n is the number of magnetosomes in the chain and R is the radius of a single magnetosome and an overall dipole moment of $n\vec{M}$, where $\vec{M}$ is the dipole moment on each

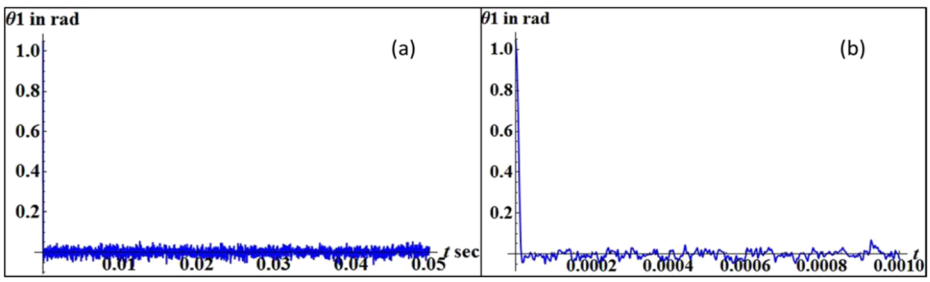

Fig. 7 (a) Variation of angle of alignment $\theta_1(t)$ of the second magnetosome as a function of time with $\theta_1(0) = \frac{\pi}{3}$ radians. (b) Expanded version of graph (a) for initial times (case 3)

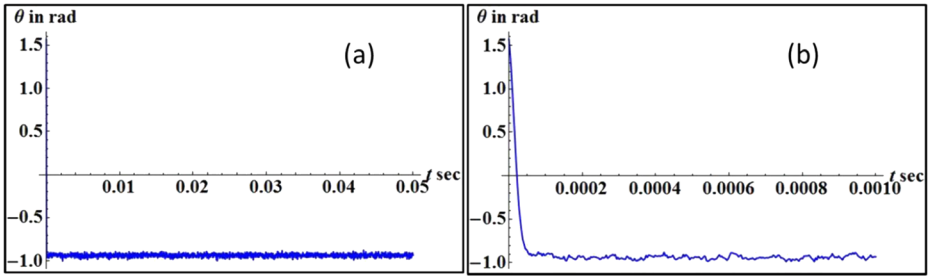

Fig. 8 Variation of angle of alignment of magnetosome $\theta(t)$ as a function of time with $\theta(0) = \frac{\pi}{2}$ radians (a) considering magnetic interaction with a neighboring dipole which is fixed in position (fixed angular position is taken as $\frac{\pi}{3}$ radians); (b) expanded version of graph (a) for initial times (case 2)

magnetosome. Fitting the time variation of the angle between the axis of the chain and the external field direction, in the small angle range, to the form given by Eq. (10), we extract relaxation times and variance values. This is plotted as a function of the number of magnetosomes as shown in Fig. 9. We find that as the number of magnetosomes increase, the relaxation time increases while the variance decreases. This indicates that increased drag has a larger effect on the orientation process than the increased magnetic moment of the aligned set of magnetosomes. However, the rate at which the relaxation time changes with the increase in the number of dipoles can be seen to vary as the number of dipoles in the aligned system increases. This could be a sensitive function of the fixed distance between the dipoles (linked to magnetosome size), individual dipole strength, and external field strength. For the parameters used here, the rate of change in the relaxation time appears to increase sharply after 12 magnetosomes. One can speculate that this factor plays a role in limiting the number of magnetosomes observed in viable MTB. The decrease in the variance with increase in the number of dipoles can, once again, be attributed to the larger drag of the system of aligned dipoles.

4 Conclusion and outlook

We have simulated the alignment process of an isolated MTB with the Earth's magnetic field direction as well as that of a single isolated magnetosome. Using experimentally measured values of the various parameters, we find that while the relaxation time of an isolated magnetosome is vastly reduced in comparison to that of the bacterium implying a faster response, the variance in the angle of orientation after alignment is larger pointing to a reduction in the robustness of alignment. We find

Table 4 σ_a^2 in the alignment process of a magnetosome interacting with a neighboring dipole with identical parameters for various values of inter dipole distance s, at a field strength of 50 μT

Inter-magnetic dipolar distance, s (in nm)	σ_a^2 (rad^2)×10^{-5}
50	28.8
75	88.7
100	215
150	776
200	1740
500	5370
1000	6651
∞ (single magnetosome)	6845

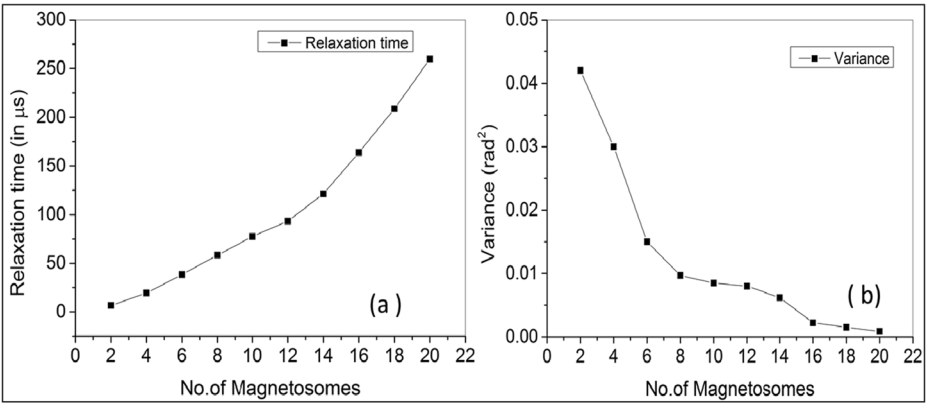

Fig.9 (a) Variation of relaxation time with number of magnetosomes arranged in a linear chain for its alignment with the Earth's magnetic field. (b) Variation of variance for this process with number of magnetosomes

that the relaxation time is vastly reduced when we allow for an interaction between the magnetosome and a neighboring one.

We also conclude that an alignment between the magnetic dipoles of a magnetosome and its neighbor is extremely likely and one can expect that the locked system of the two dipoles will respond as a unit to the external field. An increase in the number of magnetosomes in a locked linear system leads to an increase in the response time in the alignment process albeit an improvement in the robustness of alignment. This factor could be important in limiting the number of magnetosomes in a locked linear chain for optimal alignment response.

It remains to be seen how much further the alignment process is strengthened if interaction with yet another neighbor is allowed without the imposition of a linear chain structure. It is possible that the strengthening of the process saturates or even reduces beyond a certain number of dipolar interactions. Further, our simulations assume that the Earth's magnetic field and the magnetic dipoles linked with the magnetosomes lie in the same plane. We need to carry out this simulation under the most general conditions where these vectors need not be contained in the same plane. This could be initially carried out for two dipoles. We could then introduce yet another neighboring dipole in this three-dimensional scenario to study how this will alter the situation. This will take us on the path towards realizing the various factors and their relative importance in the process of magneto-sensing. Understanding the crucial factors that determine the key property of magneto-sensing in MTB could help in the design of alternate systems that are as effective in magneto-sensing but more amenable to cultivation/synthesis on a commercial scale. The simulation studies described here are an attempt to move in this direction.

Acknowledgments One of the authors (SS) is grateful to the University Grants Commission (UGC), India, for providing the Teacher fellowship. Authors are grateful to Prof. A.R. Usha Devi, Department of Physics, Bangalore University, Bengaluru, for her help and support in carrying out the simulation.

Funding One of the authors (SS) has been granted with Teacher fellowship by the University Grants Commission (UGC), India, and the fellowship number is FIP/12th Plan/KABA087. TF CODE: BA 022.

Compliance with ethical standards

Conflict of interest The authors declare no conflict of interest.

References

1. Blakemore, R.P.: Magnetotactic bacteria. Science **190**, 377–379 (1975)
2. Frankel, R.B., Blakemore, R.P., Wolfe, R.S.: Magnetite in freshwater magnetotactic bacteria. Science **203**, 1355–1356 (1979)
3. Lefèvre, C.T., Bazylinski, D.A.: Ecology, Diversity and evolution of magnetotactic bacteria. Microbiol. Mol. Biol. Rev. **77**, 497–526 (2013)
4. Abreu, F., Acosta-Avalos, D.: Biology and physics of magnetotactic bacteria. Microorganisms, M. Blumenberg, M. Shaaban, A. Elgaml, Eds. (2018). https://doi.org/10.5772/intechopen.79965
5. Bazylinski, D.A., Garratt-Reed, A.J., Frankel, R.B.: Electron microscopic studies of magnetosomes in magnetotactic bacteria. Microsc. Res. Tech. **27**, 389–401 (1994)
6. Körnig, A., Dong, J., Bennet, M., Widdrat, M., Andert, J., Müller, F.D., Schüler, D., Klumpp, S., Faivre, D.: Probing the mechanical properties of magnetosome chains in living magnetotactic bacteria. Nano Lett. **14**, 4653–4659 (2014)
7. Kiani, B., Faivre, D., Klumpp, S.: Self organization and stability of magnetosome chains – a simulation study. PLoS One **13**(1), e0190265 (2018). https://doi.org/10.1371/journal.pone.0190265
8. Ofer, S., Nowik, I., Bauminger, E.R., Papaefthymiou, G.C., Frankel, R.B., Blakemore, R.P.: Magnetosome dynamics in magnetotactic bacteria. Biophys. J. **46**, 57–64 (1984)
9. Natan, E., Vortman, Y.: The symbiotic magnetic sensing hypothesis - do magnetotactic bacteria underlie the magnetic sensing capability of animals? Mov. Ecol. **5**, 22 (2017). https://doi.org/10.1186/s40462-017-0113-1
10. Kirschvink, J.L.: Magnetite biomineralization and geomagnetic sensitivity in higher animals: an update and recommendations for future study. Bioelectromagnetics **259**, 10–23 (1989)
11. Shaw, J., Boyd, A., House, M., Woodward, R., Mathes, F., Cowin, G., Saunders, M., Baer, B.: Magnetic particle mediated magnetoreception. J. R. Soc. Interface **12**(110), 0499 (2015). https://doi.org/10.1098/risf.2015.0499
12. Vargas, G., Cypriano, J., Correa, T., Leao, P., Bazylinski, D.A., Abreu, F.: Applications of magnetotactic bacteria, magnetosomes and magnetosome crystals in biotechnology and nanotechnology: a mini-review. Molecules **23**(10), 2438 (2018). https://doi.org/10.3390/molecules23102438
13. Liu, Y., Li, G.R., Guo, F.F., Jiang, W., Li, Y., Li, L.J.: Large-scale production of magnetosomes by chemostat culture of *Magnetospirillum gryphiswaldense* at high cell density. Microb. Cell Factories **9**, 99 (2010). https://doi.org/10.1186/1475-2859-9-99
14. Nogueira, F.S., Henrique, G.P., de Barros, L.: Study of the motion of magnetotactic bacteria. Eur. Biophys. J. **4**, 13–21 (1995)
15. Volpe, G., Volpe, G.: Simulation of a Brownian particle in an optical trap. Am. J. Phys. **81**, 224–230 (2013)
16. Brown, W.F.: Thermal fluctuations of a single domain particle. Phys. Rev. **130**, 1677–1686 (1963)
17. Kong, D., Lin, W., Pan, Y., Zhang, K.: Swimming motion of rod-shaped magnetotactic bacteria: the effects of shape and growing magnetic moment. Front. Microbiol. **5**, 8 (2014). https://doi.org/10.3389/fmicb.2014.00008
18. Yan, L., Zhanga, S., Chen, P., Liu, H., Yin, H., Li, H.: Magnetotactic bacteria, magnetosomes and their application. Microbiol. Res. **167**, 507–519 (2012)

Affiliations

Savitha Satyanarayana [1,2] · Shwetha Padmaprahlada [3] · Raghunatha Chitradurga [4] · Sarbari Bhattacharya [1]

✉ Sarbari Bhattacharya
sarbari.bhattacharya@bub.ernet.in

[1] Department of Physics, Bangalore University, Bengaluru 560056, India

[2] Department of Physics, Government First Grade College, Chickballapura 562101, India

[3] Department of Physics, St. Joseph's Indian Composite PU College, Bengaluru 560001, India

[4] Department of Physics, MES Degree College, Bengaluru 560003, India